ACS APPLIED MATERIALS & INTERFACES

Research Article

www.acsami.org

Oral Delivery of Near-Infrared Quantum Dot Loaded Micelles for Noninvasive Biomedical Imaging

Zehedina Khatun,[†,§] Md Nurunnabi,[†,§] Kwang Jae Cho,[‡] and Yong-kyu Lee*[,†]

[†]Department of Chemical and Biological Engineering, Korea National University of Transportation, Chungbuk 380-702, Republic of Korea

[‡]Department of Otolaryngology, Head & Neck Surgery, The Catholic University of Korea, College of Medicine Uijeongbu St. Mary's Hospital, Kyunggi-Do 480-717, Republic of Korea

ABSTRACT: The purpose of this study is to design, develop, and characterize an optical imaging agent for oral administration. The hydrophobic, nanosized (7 nm), near-infrared (NIR) quantum dots (QDs) have been loaded into deoxycholic acid (DOCA) conjugated low molecular weight heparin (LMWH) micelles. The QD-loaded LMWH-DOCA (Q-LHD) nanoparticles have been characterized by electrophoretic light scattering (ELS) and a transmission electron microscope (TEM) which shows the average particle size was 130−220 nm in diameter. The Q-LHD nanoparticles also show the excellent stability in different pH conditions, and the release profile demonstrates the slow release of QDs after 5 days of oral administration. Concfocal laser microscopic scanning images show that the Q-LHD nanoparticles penetrate the cell membrane and are located inside the cell membrane. The real time pharmacokinetics studies show the absorption, distribution, metabolism, and elimination profile of Q-LHD nanoparticles, observed by the Kodak molecular imaging system (KMIS). This study has demonstrated that the orally administered Q-LHD nanoparticles are absorbed in the small intestine through the bile acid transporter and eliminated through the kidneys.

KEYWORDS: *heparin, quantum dot, oral delivery, biomedical imaging, biodistribution*

1. INTRODUCTION

Noninvasive molecular imaging is one of most promising areas for the biomedical and biological field to diagnosis disease and image the internal organs of the human body.[1−3] Over the last two decades, researchers have been trying to develop an optimistic and convenient imaging candidate for noninvasive imaging of the human body.[4,5] Among the imaging candidates, gold nanoparticles, iron oxide nanoparticles, and quantum dots (QDs) are the most promising for diagnosis and as carriers of drug molecules as well.[6] However, near-infrared QDs are the most promising and unique candidate for optical imaging of deep tissue, vein, and organs due to their unique properties of photo stability, narrow band gap, high luminescence, and long excitation.[7−14]

A vast numbers of research articles have reported on QDs mainly focusing on parenteral route of administration, more specifically IV administration.[15,16] In the mean time, numerous articles have reported that the QDs are not safe for human application due to the toxic effect of cadmium, which is commonly used to synthesize QDs. As QDs are known to be toxic to humans due to the elements of which they are composites of, it is assumed that the QDs show their maximum toxic effect due to IV administration. QDs could easily, rapidly, and directly reach the cells through the blood circulation through IV administration. To minimize the release of toxic elements from the QDs, several techniques have been developed and reported, such as surface modification, gold coating, ligand conjugation, and cross-linking.[17−22] We have assumed that the oral delivery of QDs could minimize and/or inhibit the toxic effect of QDs, and we have designed an oral delivery formulation.

On the other hand, oral delivery of QDs is supposed to be the best way for noninvasive imaging in the biomedical field. In our previous work, we have reported that QD-loaded heparin nanoparticle could be absorbed through the bile acid transporter of the small intestine and observed the absorption site through the optical imaging technique.[23]

As we reported previously, deoxycholic acid (DOCA) conjugated low molecular weight heparin (LMWH) absorbed in the small intestine, more specifically through bile acid transporter of ileum.[24−28] DOCA conjugated LMWH (LHD) forms micelles in aqueous solution, and hydrophobic QDs were loaded into the micelles by a solvent evaporation method. QD-loaded LHD (Q-LHD) nanoparticles were found to be absorbed through the bile acid transporter as LHD micelles were absorbed in the small intestine. In this study, we have observed fluorescence intensity, size, morphology, and stability of Q-LHD nanoparticles as well as observed the release of QDs from the Q-LHD nanoparticles in the in vitro condition. The in vitro cellular uptake study of Q-LHD nanoparticles has also

Received: April 11, 2012
Accepted: July 27, 2012
Published: July 27, 2012

been observed by a confocal laser scanning microscope (CLSM) with Caco-2 cell line in different concentrations. The brighter filed images demonstrated that the Q-LHD nanoparticles are located inside the cell membrane, but there was no fluorescence intensity in the nucleus as Q-LHD nanoparticles are unable to penetrate the nucleus membrane. The QDs loaded into DOCA conjugated LMWH nanoparticles overcame the barriers of oral delivery of naparticles which had been reported by Nie S.[29] Different dosages (2.5 and 5 mg/kg) of Q-LHD nanoparticles were orally administered to the SKH1 nude mice and observed by a Kodak molecular imaging station (KMIS) over 36 h for real time imaging and pharmacokinetics studies. The competitive oral absorption profile of Q-LHD was also observed through a noninvasive imaging technique. The organs of orally administered mice were also observed after dissecting the mice. To specifically identify the absorption position, the small intestines were separated into the duodenum, jejunum, and ileum and imaged. The formation of the Q-LHD nanoparticle has been shown as a schematic presentation in Figure 1.

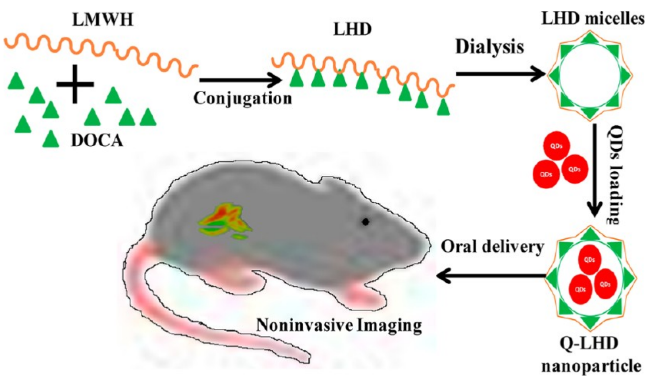

Figure 1. The scheme represents the process of Q-LHD nanoparticle formation. The Q-LHD nanoparticles were orally administered and used for noninvasive imaging of the GI tract.

The competitive oral absorption studies confirmed that the Q-LHD nanoparticle could only be absorbed through interaction with bile acid transporter. This technique could also be applied for abdominal, heart, liver, and kidney imaging noninvasively.

2. MATERIALS AND METHODS

2.1. Materials. Low molecular-weight heparin (Fraxiparine or LMWH, MW: 5000 Da) was obtained from Mediplex Corp. (Seoul, Korea). Sodium deoxycholic acid (DOCA), dimethyl formamide (DMF), triethyl amine (TEA), 4-nitrophenylchloroformate, absolute ethanol (EtOH), formamide, 4-methylmorpholine, ethylenediamin, dimethyl sulfoxide (DMSO), *N*-hydroxysuccinimide (NHS), *N*,*N*′-dicyclohexylcarbodiimide (DCC), trioctylphosphine oxide (TOPO), hexadecylamine (HAD), cadmium oxide, selenium powder, and dodecanoic acid were obtained from Sigma−Aldrich, Co. (St. Louis, MO). Caco-2 cells were collected from the Korea cell bank (Seoul, Korea). Cell culture reagents, including fetal bovine serum (FBS) and minimum essential medium (MEM), were purchased from Sigma−Aldrich, Co. (St. Louis, MO); sodium bicarbonate ($NaHCO_3$) was purchased from OCI Co., Ltd. (Seoul, Korea). *N*-2-Hydroxylethyl-plperazine-*N*′-4-butanesulfonic acid (HEPES) was purchased from Biosesang (Seoul, Korea), and penicillin−streptomycin was purchased from Gibco BRL (Carlsbad, CA). 3-(4,5-Dimethylthiazol-2-yl)-2,5-diphenyl tetrazolium bromide (MTT) was purchased from Amresco, Inc. (Solon, OH). A Coatest Heparin FXa assay kit was purchased from Chromogenix (Milano, Italy).

2.2. Synthesis of Low Molecular Weight Heparin and Deoxycholic Acid Conjugates (LHD). The chemical conjugates of LMWH and DOCA were synthesized by conjugating the hydroxyl group of DOCA with the carboxylic group of LMWH according to our previous method.[22−27,29,30] For amination of deoxycholic acid (DOCA, 0.77 mmol), 5 mL of DMSO was reacted with 4-nitrophenyl chloroformate (4-NPC, 3.86 mmol) and triethylamine (4.63 mmol) for 6 h at room temperature. After reaction, the precipitant was removed by a 0.45 μm filter membrane. The filtrate was extracted with 25 mL of ethyl acetate and 25 mL of water. The crude product from aqueous solution was washed with ethyl acetate three times, and then, DOCA carbonate was obtained as a powder after freeze-drying. To obtain aminated DOCA, DOCA carbonate was reacted with 4-methylmorpholine (1.10 mmol) and ethylenediamine (0.05 mmol) overnight at room temperature. The product was concentrated by rotary evaporation and then precipitated by adding acetonitrile.

For preparation of the LMWH-DOCA conjugate, LMWH (0.02 mmol) was dissolved in water and adjusted to pH 5.0 by adding 0.1 M HCl solution. The solution was mixed with 1-ethyl-3-(3-dimethylaminopropyl) carbodiimidehydrochloride (EDAC) (0.04 mmol), NHS (0.04 mmol), and aminated DOCA (0.044 mmol). After 30 min, the mixture was dialyzed (MWCO: 2000) against water to remove unreacted NHS, EDAC, and aminated DOCA ($DOCA-NH_2$). The final product, LMWH-DOCA (LHD), was obtained and stored at 4 °C after freeze-drying.

2.3. Synthesis of Near-Infrared Quantum Dots. To synthesis near-IR QDs (CdTe/CdSe), a mixture of CdO (0.10 mmol), 4,4′-oxydiphthalic dianhydride (ODPA) (0.205 mmol), and trioctylamine (TOA) (10 mL) was heated to a clear solution at 300 °C under argon gas. A solution of tellurium (0.2 mmol, dissolved in 0.475 g of trioctyl phosphate, TOP) was then quickly injected into the hot solution, and the reaction mixture was allowed to cool to 250 °C to allow growth of CdTe nanocrystals. To monitor the reaction process, aliquots were removed at different reaction times and their UV−vis was measured. The reaction was stopped when the nanocrystal reached the desired size. To avoid oxidation, aliquots were mixed with anhydrous chloroform and stored under argon gas before purification. For the CdTe/CdSe core/shell, CdTe QDs (0.02 g) were dispersed in TOPO (2 g) and HAD (2 g) before being heated to 190 °C. In addition, $CdCl_2$ (0.1 g) was dissolved in TOP (3 mL) with gentle heating. After being cooled to room temperature, the resulting 0.2 M solution was mixed with Se (2.5 mL, 0.2 M in TOP) after which it was injected using a syringe pump into a reaction flask containing the core nanocrystals at 190 °C within 30 min. The crystals were then annealed at 170 °C for an additional 30 min.

Core/shell nanospheres of various sizes were obtained by adjusting the concentrations of $CdCl_2$ and Se in TOP as well as the corresponding injection periods. The prepared CdTe/CdSe QDs were further purified by centrifugation, and the precipitation process was repeated several times.

2.4. Loading the Quantum Dots and Characterizations. For loading of QDs into LHD nanoparticles, 50 mg of LHD was dissolved in 2.5 mL of formamide; 0.5, 0.4, and

dx.doi.org/10.1021/am301048m | ACS Appl. Mater. Interfaces 2012, 4, 3880−3887

Table 1. Characteristics of Near-IR QD-Loaded LHD Nanoparticles (Q-LHD)[a]

sample	LHD (mg)	QDs (0.112 μM/mL)	loading efficiency (%)	average diameter (nm)	Zeta potential (mV)	emission (nm)	fluorescence intensity (RFU)
LHD				105 ± 19.09	−68 ± 13.58		
QDs				7 ± 1.65	25 ± 4.42	670	3250.67
Q-LHD/0.5	50	0.5 mL	89	220 ± 26.32	−7.3 ± 3	675	1720.58
Q-LHD/0.4	50	0.4 mL	93	157 ± 32.16	−16.4 ± 2	675	1620.23
Q-LHD/0.3	50	0.3 mL	96	132 ± 21.64	−36.8 ± 3	675	1385.23

[a]The table represents particle size, loading efficiency, zeta potential, emission, and fluorescence intensity of Q-LHD nanoparticles. (All data (n = 3) represent mean ± SD.)

0.3 mL (0.112 μM/ml) of QD solution (chloroform) were added into the LHD solution (Table 1). The mixture was vigorously stirred to facilitate the hydrophobic QDs to be loaded into the core of the LHD micelles. Chloroform was evaporated after overnight stirring in an open flask, and the remaining chloroform was evaporated under reduced pressure by a vacuum evaporation technique. The solution was dialyzed against water for 2 days to exchange the organic solvent with an aqueous solution. The free unloaded hydrophobic QDs became aggregated and precipitated in the aqueous medium. The solution was filtered by a hydrophobic filter to remove the precipitated QDs. Finally, the product was dried for 48 h by a freeze-dryer. The Q-LHD nanoparticles were characterized by electrophoretic light scattering (ELS) to measure average size distribution and zeta-potentials, transmission electron microscope (TEM) to observe the size and shape, and varioskan flash to observe the fluorescence intensity and emission.

2.5. In Vitro Release Study and Stability. For the in vitro release study, the required amount of Q-LHD nanoparticles was taken into a dialysis tube (Spectra/Por Float A-Lyzer; MWCO: 2000 g/mol; diameter: 10 nm; volume: 10 mL). The dialysis tube, containing 3 mL of a Q-LHD (1 mg/mL) nanoparticle solution, was introduced into the in vitro release medium containing 50 mL of buffer solutions (pH of 1.5, 5, 7.4, and 9) at 100 rpm. All the assemblies were kept at constant room temperature (37 °C). The concentration of QDs from the Q-LHD was collected at a predetermined time and measured by UV. The percentage of QDs release was calculated using the equation given below:

$$\%\text{ of QDs release} = \{1 - \text{absorbance } (t)/\text{absorbance } (t_0)\} \times 100$$

In the above equation, t indicates absorbance is measured time, and t_0 is the initial time.

At the same time, the intensity of fluorescence was also measured by variskan flash to observe the variation of fluorescence intensity based on pH of the solvent. The Q-LHD sample was dissolved in aqueous solvent with different pH: 1.5, 5, 7.4, and 9. To investigate the stability of Q-LHD nanoparticles, we measured the changes in the fluorescent intensity of Q-LHD nanoparticles in an aqueous solution over time (up to 7 days). Samples (200 μL) were collected from the stock solution and analyzed by a microplate reader.

2.6. In Vitro Cytotoxicity Test. The cytotoxicities of the Q-LHD conjugates were examined using the human epithelial colorectal adenocarcinoma cell line, Caco-2 cell line (Korea cell bank). The Caco-2 cells were cultured at 37 °C in a humidified atmosphere containing 5% CO_2 in a MEM medium with 10% fetal calf serum. The cells (5 × 10^4 cells/mL) grown as a monolayer were harvested by 0.25% trypsin−0.03% EDTA solution. The cells (200 μL) in their respective media were seeded in a 96-well plate and preincubated for 24 h before the assay. The cell viability of the Caco-2 cell lines was evaluated in the different groups by the MTT colorimetric assay kit. The Caco-2 cells were placed in the 96-well plates and incubated for 24 h. After suction, the complete medium and the sample were placed and again incubated in the referred condition. MTT solution aliquots at 5 mg/mL in phosphate buffered saline (PBS) were prepared followed by culture incubation with this solution at 5% in the culture medium for 4 h in an incubator with a moist atmosphere of 5% CO_2 and 95% air at 37 °C. Afterward, 100 μL of the MTT solubilizing solution was added to each well. After smooth and slow shaking for 15 min, the MTT colorimetric assay absorbance was measured at a 570 nm wavelength with a Varioskan flash and was directly proportional to the cell viability. The cell viability was expressed as a percentage. It was calculated by the following equation.

$$\text{cell viability } (\%) = (\text{sample absorbance}/\text{control absorbance}) \times 100$$

2.7. In Vitro Cellular Uptake. For a cellular uptake study of Q-LHD nanoparticle, the nanoparticles were incubated with Caco-2 cell line. The Caco-2 cells were cultured at 37 °C in a humidified atmosphere containing 5% CO_2 in a MEM medium with 10% fetal calf serum. The cells (5 × 10^4 cells/mL) grown as a monolayer were harvested by 0.25% trypsin−0.03% EDTA solution. The cells (200 μL) in their respective media were seeded in an 8-well plate and preincubated for 24 h before the assay. Different concentrations of the Q-LHD nanoparticles were added with the 8-well plate and incubated for 1 h before observation by a confocal laser scanning microscope. The wells were washed 5 times by PBS to remove the free particles from the outside of the cell membrane. A 4% formaldehyde solution was added to preserve the cell, and it was observed by confocal laser scanning microscope (CLSM)to get a noise free clear cellular image.

2.8. Noninvasive Optical Imaging Study. Six to seven week-old SKH1 female nude mice (average body weight of 21−25 g) were purchased from Orient Bio INC., (Seoul, Korea) and maintained under specific pathogen-free conditions. All experiments were approved by institutional guidelines of the Institutional Animal Care and Use Committee (IACUC) of the Catholic University of Korea College of Medicine in accordance with the NIH Guidelines. For in vivo imaging studies, SKH1 mice were administered 2.5 and 5 mg/kg of Q-LHD nanoparticles through oral gavage. Mice were anesthetized with ketamine (87 mg/kg, Virbac Laboratories, France) and xylazine (13 mg/kg, Kepro B.V., Netherland) via intraperitoneal injection. In vivo mice images were taken by a time-domain diffuse optical tomography system. In experimental section, mice were placed on the imaging platform.

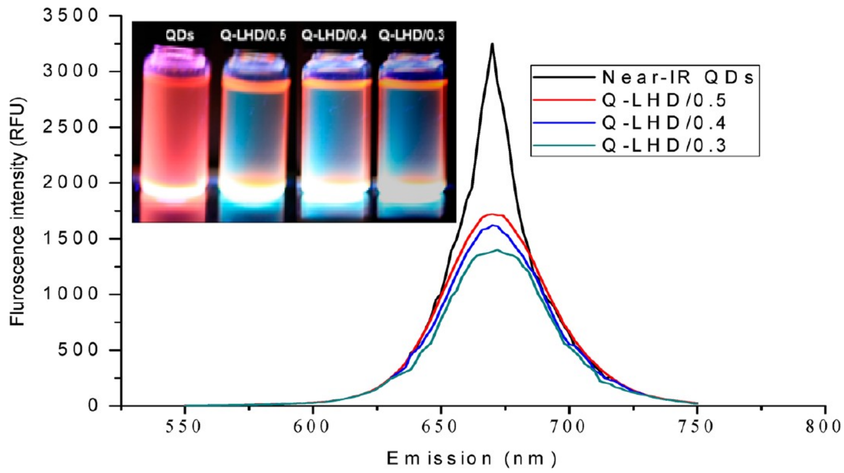

Figure 2. Fluorescence intensity of near-IR QDs and Q-LHD nanoparticles. Fluorescence intensity reduced due to load into the LHD micelles and also varied depending on the loaded amount of QDs. The visualized image (inset) of each sample was also shown.

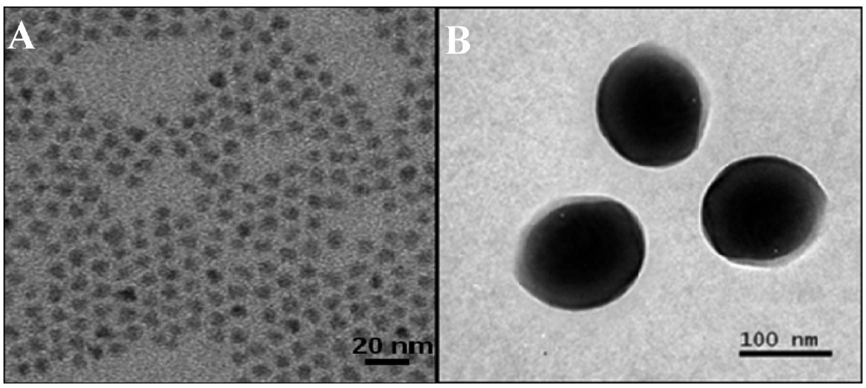

Figure 3. TEM images of near-IR QDs (A) represent that the size was 5−7 nm in diameter and the size of Q-LHD nanoparticles (B) was ∼130 nm in diameter.

Images were taken at 2, 4, 6, 8, 10, 12, and 24 h post injection. The 3D scanning region of interest was selected using bottom-view charge-coupled device (CCD). All images were taken using the Kodak in vivo imaging system (4000MN PRO, Kodak, USA).

2.9. Competitive Oral Absorption Test of Q-LHD. To observe the competitive oral absorption profile Q-LHD, taurocholic acid (TCA) (which is a commercially available bile acid) was orally administered to the six to seven week-old SKH1 female nude mice (25−26 g) which were purchased from Orient Bio INC., (Seoul, Korea). TCA was dissolved in 10% DMSO/90% PBS solvent (W/W) and orally administered to mice at different dosages (0, 25, and 50 mg/kg). Q-LHD was dissolved in PBS and administered orally at 2.5 mg/kg after 1.5 h of TCA administration. The nude mice were imaged by KMIS after 8 h of Q-LHD administration.

2.10. Inductively Coupled Plasma-Mass Spectrometry (ICP-MS) Analysis. To determine the intracellular concentrations of Cd^{2+} ion, the mice were dissected and organs (heart, liver, lung, kidney, ileum, duodenum, jejunum) were isolated from the mice, washed with PBS, and then weighed. Afterward, the organs were homogenized by a homogenizer (FM300 Digital High Shear Homogenizer, Shanghai, China (Mainland)), followed by ultra sonication (VCX 500 (500 W) and VCX 750 (750 W), USA) for 2 min. Furthermore, the extracted tissue was ultra centrifuged at 25 000 rpm for 180 min to separate the tissue from the liquid portion. The liquid portion was analyzed by ICP-MS (Nexon-300, ParkinElmer, USA) to measure the content of cadmium ions.

3. RESULTS AND DISCUSSION

3.1. Synthesis and Characterization. Bile acid DOCA has been chemically conjugated with LMWH according the previously reported method.[23] Conjugation between the carboxyl groups of LMWH and the amine groups of DOCA was confirmed by the presence of signals at 8.0−8.2 ppm in the ^{1}H NMR spectrum. The purities of the conjugates were analyzed by liquid chromatography (LC). The average particle size and morphology of both QDs and Q-LHD nanoparticles were measured to observe the particle size distribution, shape, and morphology of the particles. The average sizes of LHD, QDs, and Q-LHD were 105 ± 19.09, 7 ± 1.65, and 132−220 nm in diameter, respectively, measured by ELS. The size distribution, zeta potential, and fluorescence intensity of Q-LHD nanoparticles were varied regarding the loaded amount of QDs (Table 1). Fluorescence intensity of QDs, Q-LHD/0.5, Q-LHD/0.4, and Q-LHD/0.3 were measured to observe the variation of intensity regarding the loaded amount of QDs into the LHD micelles (Figure 2). The average size of Q-LHD nanoparticles also increased simultaneously due to increasing the loaded amount of QDs. The data demonstrated that the fluorescence intensity and size distribution of Q-LHD was directly proportional to the loaded amount of QDs. TEM images show the size of the near-IR QDs and Q-LHD

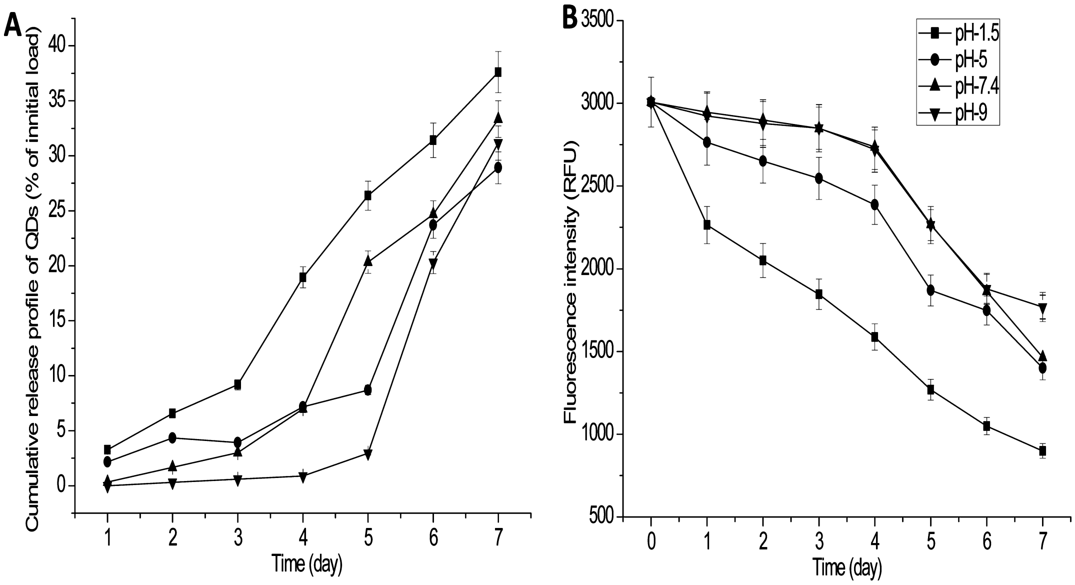

Figure 4. In vitro release profile of QDs from Q-LHD nanoparticle (A) and stability of fluorescent intensity (B) of QDs from Q-LHD nanoparticles observed at different buffer conditions for 7 days.

nanoparticles; the average particle sizes were 7 and 130 nm in diameter, respectively (Figure 3). The size of the Q-LHD nanoparticles varied depending on the loaded amount of hydrophobic QDs loaded into the LHD micelles. The Q-LHD/0.5 has been selected for in vitro and in vivo studies, which is termed Q-LHD nanoparticles in this Article.

Generally, the surface of a heparin molecule is highly negative in charge. The negative charges tend to decrease after conjugation with DOCA and dramatically decreased after QDs were loaded into the LHD micelles (Table 1). The results demonstrate that the negative charges were neutralized by the positive charge of DOCA and QDs. This effect also enhances the absorption of Q-LHD nanoparticles through the GI tract, as heparin itself is not absorbed due to a highly negative charged surface.

3.2. In Vitro Release Study. The release profile of QDs is a very important issue for the biological application of Q-LHD. It is possible to show toxicity due to the release of QDs from the Q-LHD nanoparticle. Severe toxicity may arise if the QDs remain in the human body for a long time. An in vitro release test of the Q-LHD nanoparticles was conducted to measure the release profile of QDs from the LHD nanoparticles over time (Figure 4a). The results of the release test showed that a negligible amount or very few QDs were released from the Q-LHD nanoparticles for up to 5 days at pH 7.4 and 9; the released amount was about 5% of the total loaded amount of QDs into the LHD micelle, but after 6 days of observation, the release of QDs dramatically increased (more than 20%). On the other hand, the release of QDs was higher in the cases of pH 1.5 and 5, compared to that of pH 7.4 and 9. The reason for a higher amount of QDs released at the first day is the damage to the surface of nanoparticles in an acidic environment (pH 1.5 and 5). The release of QDs could also be enhanced in the stomach during an in vivo study due to a highly acidic environment.[31] The results demonstrated that QDs start to release from the core of the Q-LHD nanoparticle after 5 days due to degradation of the micelles.

The fluorescent stability data demonstrated that the intensity of Q-LHD nanoparticles was almost stable for up to 5 days until intensity started to decrease. Release of QDs from the core of Q-LHD nanoparticles is the principle reason for the decrease of fluorescent intensity, but there are also some other specific reasons the fluorescence effect of QDs decreased; such as photo bleaching, oxidation by water, and damage of fluorescent intensity in an acidic environment (Figure 4b). The results expressed that the acidic environment (pH 1.5 and 5) could degrade the LHD micelles and induce the release of QDs from the core of micelles, resulting in released QDs and loss of fluorescence intensity in aqueous acidic medium. Recently, Mo et al. reported that pH of the dilution solvent directly affects both fluorescence and absorbance of QDs.[32] Both the fluorescence and absorbance of Q-LHD were decreased in lower pH (pH 1.5 and 5) than that of higher pH (pH 7.4 and 9).

3.3. In Vitro Cytotoxicity Test. To assess the comparative cytotoxicity of Q-LHD, different concentrations (0.1, 1, 10, 50, and 100 μg/mL) of samples were added with Caco-2 cell line and incubated for various durations (24 and 48 h). Overall, MTT assay indicates that cytotoxic effects were not significant because cell viability was still in the range from 80 to 95% during the 24 h incubation. After the 48 h incubation, the cell viability of the Caco-2 cells was still maintained over 60% after treatment with Q-LHD; there was no observation of IC_{50} values in the range of 0.1−100 μg/mL (Figures 5). Therefore, we believe that the effect of Q-LHD on the cell viability and metabolic activities was not numerically significant.

3.4. In Vitro Cellular Uptake. Different concentrations (100, 50, and 20 μg/mL) of Q-LHD nanoparticle were incubated with Caco-2 cell line for 1 h at 37 °C and 5% CO_2. The images were captured by a confocal laser scanning microscope (CLSM) after washing 5 times with PBS to remove free particles from the wells which are located outside of the cells. Q-LHD nanoparticles were taken up by Caco-2 cells and visually observed by CLSM to measure the penetration of nanoparticles and their position inside the cell membrane. The brighter portion of the cells indicates that the Q-LHD nanoparticles were located in the cell membrane, and the black dark spot indicates the nucleolus of the cells where

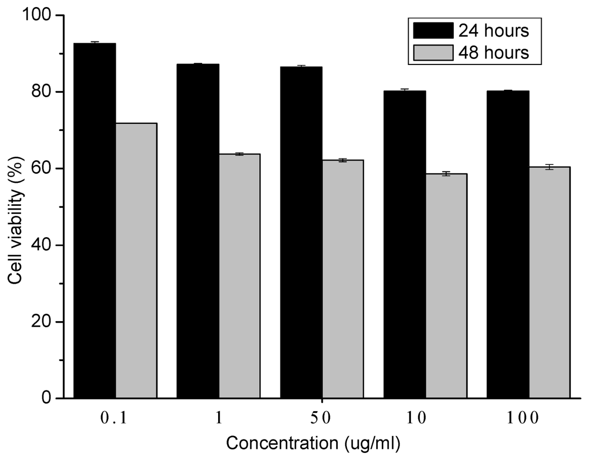

Figure 5. In vitro cytoxicity data shows the incubation for 24 h; Q-LHD nanoparticles do not show any mentionable toxic effect on cells as the cell viability was higher than 80%, but the cell viability was around 60% with 48 h of incubation.

the Q-LHD could not reach. From the magnified view of cell images, it was also observed that some of the Q-LHD nanoparticles were located on the surface of cell; these may enter into the cell membrane if the incubation period is extended. The in vivo cellular uptake study in Caco-2 cell line may confirm the absorption of the Q-LHD through oral delivery. The images for lower concentration (20 μg/mL) have shown that the quantity of survival cells is higher than the images of cells with higher concentrations (100 and 50 μg/mL), whereas the fluorescence intensities were almost the same for all concentrations (Figure 6). The results also demonstrated that the higher concentration may induce toxicity of Q-LHD nanoparticles and decrease cell viability. However, the lower concentration of Q-LHD nanoparticles is also able to penetrate the cell membrane of Caco-2 cells.

3.5. Real Time Biodistribution Study. The absorption profile of Q-LHD by the GI tract was further monitored by the Kodak molecular imaging system (KMIS). All auto fluorescence was removed by the reference filter, and the real fluorescence was captured by the region of interest (ROI). Q-LHD was administered orally to the nude mice for frequent noninvasive imaging. The images were taken up to 36 h after oral administration of dosages of 5 and 2.5 mg/kg. The signal of QDs was found around the stomach after 2 h of oral administration (Figure. 7). After 8 h of oral administration, Q-LHD reached into the small intestines, more specifically, the duodenum, jejunum, and ileum. Although the product started to be excreted from the stomach at 24 h in the case of the 2.5 mg/kg dosage, maximum accumulation of the product was shown in the small intestines at 5 mg/kg dosage. The data may demonstrate slow absorption of the product at a higher dosage. Thirty-six hours post administration, the entire product had been eliminated from the body at 2.5 mg/kg, whereas a strong signal was present in the case of the 5 mg/kg dosage. The noninvasive fluorescence imaging data indicates the lower dosage could be safer and have more potential for real time noninvasive optical imaging than that of the higher dosage. Whole body imaging of mice was also done by KMIS to observe the biodistribution of Q-LHD nanoparticle. The optical image clearly visualized that the nanoparticle is located in the lung, heart, liver, spleen, and kidneys, whereas the fluorescence was also found in the stomach (Figure 7C).

3.6. Competitive Oral Absorption Profile of Q-LHD. Highly potent bile acid TCA was orally administered at different dosages (0, 25, and 50 mg/kg) to the nude mice. After 1.5 h of TCA administration Q-LHD (2.5 mg/kg) was also orally administered to the same mice. It is assumed that the TCA is bound with the bile acid transporter of the small intestine and occupied by the mean time. The binding efficacy of orally administered Q-LHD depends on the available free

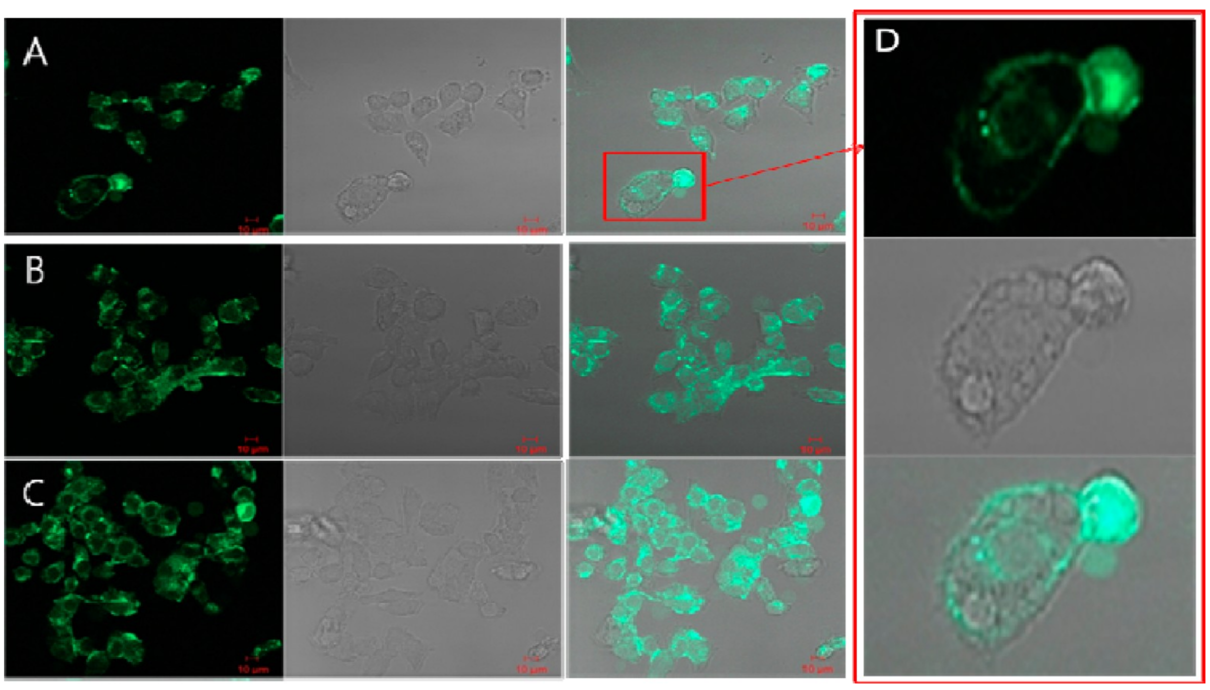

Figure 6. Confocal laser scanning microscopic images show the cellular uptake of Q-LHD nanoparticles. Each concentration of Q-LHD nanoparticles in Caco-2 cells was controlled to 20 μg/mL (A), 50 μg/mL (B), and 100 μg/mL (C) and incubated for 1 h.

dx.doi.org/10.1021/am301048m | *ACS Appl. Mater. Interfaces* 2012, 4, 3880−3887

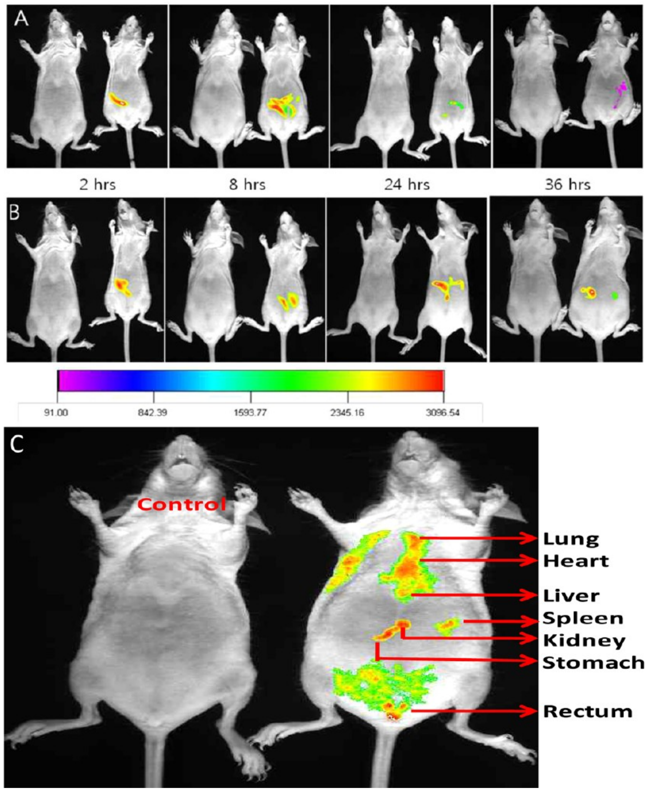

Figure 7. Noninvasive optical imaging of QD-loaded LHD for 2.5 mg/kg (A) and 5 mg/kg (B); the absorption sites were captured by region of interest. The whole body imaging data shows the Q-LHD nanoparticles accumulated in the lung, heart, liver, spleen, and kidneys and also excreting through the rectum (C).

bile acid transporter in the small intestinal surface area after binding with TCA. After 8 h of oral administration, the noninvasive imaging figures of mice, which were not administered TCA, show the Q-LHD located in the small intestinal area and stronger fluorescence intensity compared to that of the mice which were previously administered TCA (Figure 8). The results demonstrate that the entire Q-LHD could interact with bile acid transporter when those are not

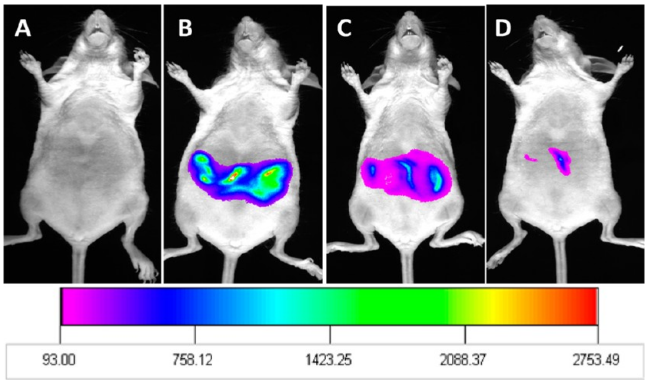

Figure 8. Competitive oral absorption profile of the Q-LHD nanoparticle. Control mice were only administered water (A); experimental mice were administered only Q-LHD (2.5 mg/kg) (B), administered both Q-LHD (2.5 mg/kg) and TCA (25 mg/kg) (C), or administered both Q-LHD (2.5 mg/kg) and TCA (50 mg/kg) (D). Noninvasive images were taken 8 h after the oral administration of Q-LHD nanoparticles.

occupied, but a portion of Q-LHD could only bind with the free bile acid receptor when the mice were previously administered with a lower dosage of TCA (25 mg/kg). No fluorescence intensity was observed from the mice which had previously been administered 50 mg/kg of TCA, the reasoning is that no free bile acid transporter was available to bind with the Q-LHD nanoparticle. The nonabsorbed Q-LHD nanoparticles could directly be eliminated from the GI tract through the excretion process. The results demonstrate that Q-LHD nanoparticles could only be absorbed through bile acid transporter as it had been conjugated with DOCA.

3.7. Analysis of Cadmium Ion by ICP-MS. The collected extract from the organs were analyzed by inductively coupled plasma mass spectroscopy (ICP-MS) to observe the content of cadmium ions in the organs. Concentration of cadmium in the kidney, liver, lung, heart, ileum, duodenum, and jejunum were measured by ICP-MS and expressed in μg/g tissue in Figure 9.

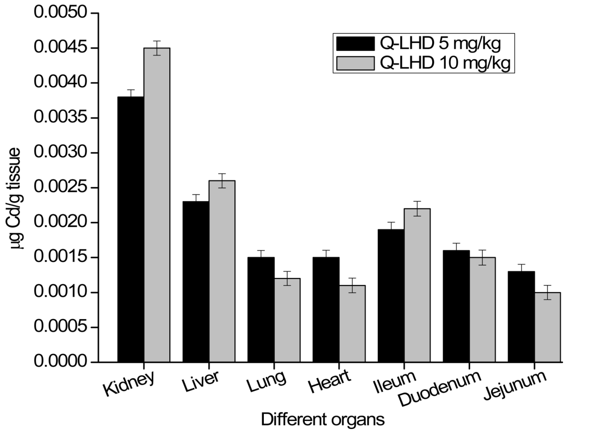

Figure 9. . ICP-MS data shows the biodistribution of quantum dots (Cd per μg of tissue) in different organs of mice. The observation was performed after 36 h of oral delivery of the Q-LHD nanoparticles. The data are plotted as mean $\pm$ SD (n = 4).

The results demonstrate that both the 5 and 10 mg/kg dose show a negligible amount of Cd^{2+} content in each and every organ. The maximum concentration of Cd^{2+} ion was observed in kidney which is also very low, 3.5 $\pm$ 0.06 and 4.5 $\pm$ 0.1 ng/mg, respectively, for 5 and 10 mg/kg dose. The results could provide adequate evidence that the Q-LHD nanoparticle is rapidly removed from the body as a very negligible amount was contained in the organs, though more studies are required to prove complete removal of the QDs from the animal body and the mechanism.

4. CONCLUSIONS

Oral delivery of imaging agent could play an essential role in minimizing the toxic effects which are usually observed in the IV administration of QDs. There is a promising opportunity for oral administration of QDs, especially for noninvasive optical biomedical imaging and pharmacokinetic studies of any orally administered drug. The bile acid DOCA enhances absorption of LMWH as well as QDs which gives optical properties for the noninvasive imaging the deep tissues. The competitive absorption profile also provided sufficient evidence to prove the bile acid transporter dependent absorption of Q-LHD. The optical fluorescence images of mice demonstrated that the Q-LHD nanoparticles distribute throughout the body after absorption through the bile acid transporter in the small

dx.doi.org/10.1021/am301048m | ACS Appl. Mater. Interfaces 2012, 4, 3880−3887

intestines. The Q-LHD nanoparticles were also assumed to be eliminated from the biological system after 72 h after oral administration, as the fluorescence signal was not observed. This technique could be widely applied for noninvasive biomedical imaging of deep tissue and organ through oral delivery of QDs.

AUTHOR INFORMATION

Corresponding Author

*Tel: +82-43-841-5224. Fax: +82-43-841-5220. E-mail: leeyk@cjnu.ac.kr.

Author Contributions

[§]These authors contributed equally.

Notes

The authors declare no competing financial interest.

ACKNOWLEDGMENTS

This research was supported by the Basic Science Research Program through the National Research Foundation of Korea (NRF) funded by the Ministry of Education, Science and Technology (2010-0021427).

REFERENCES

(1) Massoud, T. F.; Gambhir, S. S. *Genes Dev.* **2003**, *17*, 545.
(2) Sahoo, S. K.; Parveen, S.; Panda, J. J. *Nanomedicine* **2007**, *3*, 20.
(3) Hong, H.; Zhang, Y.; Sun, J.; Cai, W. *Nano Today* **2009**, *4* (5), 399.
(4) De, A.; Yaghoubi, S. S.; Gambhir, S. S. *Gene Ther. Protoc.* **2008**, *433*, 177.
(5) Cross, S. E.; Roberts, M. S. *Curr. Drug Delivery* **2004**, *1*, 81.
(6) Vlerken, L. E.; Amiji, M. M. *Expert Opin. Drug Delivery* **2006**, *3* (2), 205.
(7) Chan, W. C. W.; Maxwell, D. J.; Gao, X.; Bailey, R. E.; Han, M.; Nie, S. *Cur Opin. Biol.* **2002**, *13*, 40.
(8) Biju, V.; Itoh, T.; Anas, A.; Sujith, A.; Ishikawa, M. *Anal. Bioanal. Chem.* **2008**, *391*, 2469.
(9) Ciarlo, M.; Russo, P.; Cesario, A.; Ramella, S.; Baio, G.; Neumaier, C. E.; Paleari, L. *Recent Pat. Anti-Cancer* **2009**, *4*, 207.
(10) Du, Y.; Xu, B.; Fu, T.; Cai, M.; Li, F.; Zhang, Y.; Wang, Q. *J. Am. Chem. Soc.* **2010**, *132* (5), 1470.
(11) Jorge, P.; Martins, M. A.; Trindade, T.; Santos, J. L.; Farahi, F. *Sensors* **2007**, *7*, 3489.
(12) Vivero-Escoto, J. L.; Huang, Y.-T. *Int. J. Mol. Sci.* **2011**, *12* (6), 3888.
(13) Drbohlavova, J.; Adam, V.; Kizek, R.; Hubalek, J. *Int. J. Mol. Sci.* **2009**, *10*, 656.
(14) Manzoor, K.; Johny, S.; Thomas, D.; Setua, S.; Menon, D.; Nair, S. *Nanotechnology* **2009**, *20*, 1.
(15) Jong, W. H. D.; Borm, P. J. A. *Int. J. Nanomed.* **2008**, *3* (2), 133.
(16) Prakash, U. R. T.; Thiagarajan, P. *Res. Biotechnol.* **2011**, *2* (3), 1.
(17) Wani, M. S.; Hashim, M. A.; Nabi, F.; Malik, M. A. *Adv. Chem. Phys.* **2011**, *2011*, 1.
(18) Hoshino, A.; Hanada, S.; Yamamoto, K. *Arch. Toxicol.* **2011**, *85*, 707.
(19) Liang, X.-J.; Chen, C.; Zhao, Y.; Jia, L.; Wang, P. C. *Curr. Drug Metab.* **2008**, *9* (8), 697.
(20) Yang, Z.; Liu, Z. W.; Allaker, R. P.; Reip, P.; Oxford, J.; Ahmad, Z.; Ren, G. *J. R. Soc. Interface* **2010**, *7*, 411.
(21) Ferro-Flores, G.; Ramírez, F. M.; Meléndez-Alafort, L.; Santos-Cuevas, C. L. *Mini-Rev. Med. Chem.* **2010**, *10*, 87.
(22) Buzea, C.; Blandino, I. I. P.; Robbie, K. *Biointerphases* **2007**, *2*, 17.
(23) Khatun, Z.; Nurunnabi, M.; Cho, K. J.; Lee, Y.-k. *Carbohydr. Polym.* **2012**, http://dx.doi.org/10.1016/j.carbpol.2012.07.016.
(24) Kim, S. K.; Lee, D. Y.; Kim, C. Y.; Nam, J. H.; Moon, H. T.; Byun, Y. *J. Controlled Release* **2007**, *123*, 155.
(25) Park, J. W.; Kim, S. K.; Al-Hilal, A. T.; Jeon, O. C.; Moon, H. T.; Byun, Y. *Biotechnol. Bioprocess Eng.* **2010**, *15*, 66.
(26) Lee, D. Y.; Kim, S. Y.; Kim, Y. S.; Son, D. H.; Nam, J. H.; Kim, I. S. *J. Controlled Release* **2007**, *118*, 310.
(27) Kim, S. K.; Kim, K.; Lee, S.; Park, K.; Park, J. H.; Kwon, I. C.; Choi, K.; Kim, C.-Y.; Buyn, Y. *J. Pharm. Biomed. Anal.* **2005**, *39*, 861.
(28) Lee, D. Y.; Lee, S. W.; Kim, S. K.; Lee, M.; Chang, H. W.; Moon, H. T.; Buyn, Y.; Kim, S. K. *Pharm. Res.* **2009**, *26*, 2667.
(29) Mohs, A. M.; Duan, H; Kairdolf, B. A.; Smith, A. M.; Nie, S. *Nano Res.* **2009**, *2*, 500−508.
(30) Kim, S. K.; Kim, K.; Lee, S.; Park, K.; Park, J. H.; Kwo, I. C. *J. Pharm. Biomed. Anal.* **2005**, *39*, 861.
(31) Lindahl, A; Ungell, A. L.; Knutson, L; Lennernäs, H. *Pharm. Res.* **1997**, *14*, 497−502.
(32) Mo, Y.-m.; Tang, Y.; Gao, F.; Yang, J.; Zhang, Y.-m. *Ind. Eng. Chem. Res.* **2012**, *51*, 5995−6000.